

Dissipative dark matter and the rotation curves of dwarf galaxies

R. Foot¹

*ARC Centre of Excellence for Particle Physics at the Terascale,
School of Physics, University of Melbourne,
Victoria 3010 Australia*

There is ample evidence from rotation curves that dark matter halos around disk galaxies have nontrivial dynamics. Of particular significance are: a) the cored dark matter profile of disk galaxies, b) correlations of the shape of rotation curves with baryonic properties, and c) Tully-Fisher relations. Dark matter halos around disk galaxies may have nontrivial dynamics if dark matter is strongly self interacting and dissipative. Multicomponent hidden sector dark matter featuring a massless ‘dark photon’ (from an unbroken dark $U(1)$ gauge interaction) which kinetically mixes with the ordinary photon provides a concrete example of such dark matter. The kinetic mixing interaction facilitates halo heating by enabling ordinary supernovae to be a source of these ‘dark photons’. Dark matter halos can expand and contract in response to the heating and cooling processes, but for a sufficiently isolated halo could have evolved to a steady state or ‘equilibrium’ configuration where heating and cooling rates locally balance. This dynamics allows the dark matter density profile to be related to the distribution of ordinary supernovae in the disk of a given galaxy. In a previous paper a simple and predictive formula was derived encoding this relation. Here we improve on previous work by modelling the supernovae distribution via the measured UV and $H\alpha$ fluxes, and compare the resulting dark matter halo profiles with the rotation curve data for each dwarf galaxy in the LITTLE THINGS sample. The dissipative dark matter concept is further developed and some conclusions drawn.

¹E-mail address: rfoot@unimelb.edu.au

1 Introduction

Large scale structure (LSS) and measurements of the cosmic microwave background (CMB) provide strong evidence for the existence of nonbaryonic dark matter in the Universe, e.g. [1, 2, 3, 4, 5, 6, 7, 8, 9]. Dark matter, whether collisionless or collisional, provides a compelling explanation for the measured anisotropies of the CMB and the observed large scale structure. On much smaller scales, measurements of the rotation curves of disk galaxies have also yielded very convincing evidence for the existence of nonbaryonic dark matter. Indeed, galaxy rotation curves are (typically) observed to be flat at the observed edge of the galaxy, in sharp contrast to the expected Keplerian decline [10, 11, 12, 13] (see also [14] and references therein).

This asymptotic flatness is certainly an intriguing feature, yet rotation curves provide much more information. Detailed studies, especially those involving low surface brightness galaxies, e.g. [15, 16, 17] and gas rich dwarfs, e.g. [18, 19, 20], have found that the dark matter profile is generally cored (see also the review [21]) and that the shape of rotation curves are correlated with baryonic properties. There are also local such correlations observed in specific galaxies, such as the rotation curve ‘wiggle’ in NGC1560 [22, 23]. Similar conclusions have also been reached in high surface brightness spiral galaxies [24, 25, 26]. See also [27, 28, 29, 30, 31, 32] and references therein for further relevant discussions. Such features, and others (e.g. Tully-Fisher relations [33, 34]) suggests to this author that dark matter self interactions are likely to be important on small scales, cf. [35, 36, 37].

In this paper we consider a particular class of collisional dark matter, dissipative dark matter. By this we mean dark matter with strong self interactions which include dissipative particle processes involving the emission of a massless (or very light) dark bosonic particle. That is, dark matter is envisaged to have broadly similar particle properties to ordinary matter. Multicomponent hidden sector dark matter featuring a massless ‘dark photon’ (from an unbroken dark $U(1)$ gauge interaction) which kinetically mixes with the ordinary photon provides a concrete example of such dark matter [38, 39, 40, 41] (see also the review [42] for a more detailed bibliography).² The kinetic mixing interaction [52, 53, 38],

$$\mathcal{L}_{int} = -\frac{\epsilon}{2} F^{\mu\nu} F'_{\mu\nu} , \quad (1)$$

facilitates halo heating by enabling ordinary supernovae to be a source of these ‘dark photons’ [54, 55]. These dark photons can transport a large fraction of a supernova’s core collapse energy to the halo (potentially up to $\sim 10^{53}$ ergs per supernova for kinetic mixing of strength $\epsilon \sim 10^{-9}$). Dark matter halos can thereby expand and contract in response to these heating and cooling processes, but at the current epoch could (typically) have evolved to a steady state or ‘equilibrium’ configuration where heating and cooling rates locally balance.

The resulting dynamics allows the dark matter density profile to be related to the distribution of ordinary supernovae in the disk of a given galaxy. In a previous paper [56] a simple formula was derived encoding this relation which, it was argued, should approximately represent dissipative dynamics independently of the details of the particular dissipative particle physics model. This formula is highly predictive as all of the model dependence, fundamental physics etc., was able to be condensed into a single parameter, λ . It was shown that this approach could potentially explain the apparent correlations

²More generally, hidden sector dark matter models with an unbroken dark $U(1)$ gauge interaction have been quite widely discussed in the literature, e.g. [43, 44, 45, 46, 47, 48, 49, 50, 51].

between the dark matter and ordinary matter distributions in galaxies. The purpose of the present paper is to further explore this predicted halo profile of dissipative dark matter, examining all 26 dwarf galaxies in the LITTLE THINGS sample [19]. In doing so, we aim to improve on previous work by modelling the supernovae distribution via the measured UV and $H\alpha$ fluxes. This is a more direct measure of the supernovae distribution than that considered previously in [56] where a Kennicutt-Schmidt type relation [57, 58] was used to model the supernovae distribution in terms of the baryonic gas density. We also briefly consider THINGS spirals [59]. Although spirals are generally not as useful in testing halo profiles due to the much larger baryonic contribution, they are important, especially for exploring the scaling behaviour of λ .

2 Halo profile from dissipative dark matter

It has been known for some time that dissipative dark matter models can explain dark matter phenomena on large scales: LSS and CMB anisotropies [60, 61, 62]. These types of models are also consistent with other cosmological probes, such as $\delta N_{eff}(BBN)$ and $\delta N_{eff}(CMB)$ [63, 41]. The small scale structure of dark matter, especially the dark matter distribution around galaxies, has been pursued in [39, 64, 65, 66, 67, 41, 42, 56].

In this picture the halo of disk galaxies is in the form of a strongly self interacting gas of particles. In the model of [41] this gas is a plasma composed of dark electrons (F_1) and dark ions (F_2) interacting via massless dark photons, γ_D . Such a halo is dynamical and can be modelled as a fluid governed by Euler's equations, with both heating and cooling processes. As in the previous studies, we assume the existence of a kinetic mixing interaction, Eq.(1), of strength $\epsilon \sim 10^{-9}$. This small interaction results in a substantial halo heat source, with up to around half of the total core-collapse energy of ordinary supernovae converted into dark photons [54, 55, 64]. These dark photons propagate out into the halo where they can eventually be absorbed there via some interaction process, with dark photoionization a likely suspect in the specific models studied [39, 64, 65, 66, 41]. It follows that the heating rate at a particular point, P , in the halo is proportional to the product of the dark matter density and dark photon energy flux at that point: $\Gamma_{heat}(\mathbf{r}) \propto n(\mathbf{r})F_{\gamma_D}(\mathbf{r})$. The halo is dissipative, and cools via dark bremsstrahlung (and potentially other processes), which means that the cooling rate at the point, P , is proportional to the square of dark matter density: $\Gamma_{cool}(\mathbf{r}) \propto n(\mathbf{r})^2$. [The proportionality coefficients depend on the details of the dissipative particle physics, and do not need to be specified for the purposes of model independent considerations.]

Given sufficient time, a dark matter halo can evolve to a steady-state configuration where the heating and cooling rates balance at every location, $\Gamma_{heat}(\mathbf{r}) = \Gamma_{cool}(\mathbf{r})$, so that:

$$n(\mathbf{r}) \propto F_{\gamma_D}(\mathbf{r}). \quad (2)$$

The timescale of this halo evolution, τ , is presumed to be much less than the current age of the Universe. A rough estimate for this timescale is the time for which dissipative interactions would dissipate all the halo's energy in the absence of heating, i.e. $\tau \sim (3/2)n(r)T/\Gamma_{cool}$ (here T is the halo temperature). The precise value of τ is of course model dependent, but expected to be less than around a Gyr in the specific models studied [41, 42].

As discussed earlier, the flux of dark photons which govern this dynamics is expected to originate within and around core-collapse supernovae. Supernovae are the final evolutionary stages of large ($M \gtrsim 8m_\odot$) stars which are located in the galactic disk. Using

spherical coordinates and setting the presumed thin disk at $\theta = \pi/2$ (i.e. the z axis is normal to the plane of the disk) the energy flux of these dark photons at a point $P = (r, \theta, \phi)$ within an optically thin halo is given by: ³

$$F_{\gamma_D}(r, \theta, \phi) \propto \int d\tilde{\phi} \int d\tilde{r} \tilde{r} \frac{\Sigma_{SN}(\tilde{r}, \tilde{\phi})}{4\pi[r^2 + \tilde{r}^2 - 2r\tilde{r} \sin \theta \cos(\tilde{\phi} - \phi)]}. \quad (3)$$

Here, $\Sigma_{SN}(\tilde{r}, \tilde{\phi})$ is the type II supernova rate per unit area in the disk. Strictly, Σ_{SN} is some appropriately weighted average over the timescale $\sim \tau$, expected to be many orders of magnitude greater than the time between the discrete supernova events.

The dynamically driven balancing of heating and cooling rates [$\Gamma_{heat}(\mathbf{r}) = \Gamma_{cool}(\mathbf{r})$] dictates the dark matter density, via Eq.(2). That is,

$$\rho(r, \theta, \phi) = \lambda \int d\tilde{\phi} \int d\tilde{r} \tilde{r} \frac{\Sigma_{SN}(\tilde{r}, \tilde{\phi})}{4\pi[r^2 + \tilde{r}^2 - 2r\tilde{r} \sin \theta \cos(\tilde{\phi} - \phi)]}. \quad (4)$$

The proportionality coefficient, λ , depends on the dark photoionization cross section, supernovae dark photon energy spectrum, and halo properties: ionization state, composition and temperature. Evidently, there is a significant parameter degeneracy which potentially makes this kind of dark matter model extremely predictive as far as galaxy dynamics is concerned, despite the nontrivial nature of dissipative dark matter.

A critical assumption in deriving Eq.(4) is that the dark halo is able to dynamically evolve until it reaches a steady-state configuration. Naturally, this could only occur if the galaxy is sufficiently isolated and the heat source (supernova rate) is sufficiently stable. Environmental effects, such as mergers, perturbations from nearby galaxies etc. could hinder an actual galaxy from attaining this ‘equilibrium’ configuration. The degree to which a particular galaxy is perturbed away from equilibrium would depend on the size of the perturbation as well as when it occurred. Once a perturbation ceases, the galaxy can re-equilibrate on the timescale $\sim \tau$, which as mentioned above is expected to be less than a Gyr. An important class of ‘perturbed’ galaxies are those currently in a starburst phase. Starburst galaxies exhibit a rapidly varying star formation rate over the last few hundred million years. Given that ordinary supernovae are the presumed source of the dark photons which heat the halo, this then implies a rapidly changing halo heating rate [$\Gamma_{heat}(\mathbf{r}, t)$]. Such a rapidly changing halo heat source can, of course, potentially perturb the halo away from the steady-state configuration. Thus, the density profile of the dark matter halo of starburst galaxies can depart significantly from Eq.(4).

Although this discussion has been couched in terms of a specific kind of dissipative dark matter model (where halo heating is supplied by massless dark photons produced via kinetic mixing induced processes in ordinary supernovae) Eq.(4) can hold more generally. The basic assumptions are only that dark matter is dissipative, behaves as a fluid which evolves to a steady-state configuration where heating and cooling rates equilibrate (on a timescale $\tau \lesssim 1$ Gyr). It is easy therefore to envisage many other dissipative dark matter models leading to Eq.(4). For example, models where heating is transported to the halo

³Supernovae produce a flux of dark photons with an uncertain energy spectrum. In general the optical depth is a frequency (energy) dependent quantity so that in actuality the halo might only be optically thin for a range of dark photon frequencies. However these optically thin dark photons can dominate the energy transport, making the optically thin approximation potentially valid even in this case. This conclusion is also supported by the numerical work of [65, 66] where the effects of finite optical depth was considered where the uncertain dark photon supernova spectrum was modelled with a wide range of possible dark photon frequency distributions.

via massive dark photons are possible. Alternatively heating might be transported from ordinary supernovae to the halo via light scalar particles. In these scenarios, various considerations constrain the mass of the massive dark photon or dark scalar to be around ~ 10 keV. However, models with energy sources other than supernovae, e.g. ordinary main sequence stars, are unlikely given the typically stringent constraints on exotic energy loss mechanisms for such objects.

In general, the coefficient λ in Eq.(4) will depend on the position, r, θ, ϕ and can be model dependent. Such spatial variation of λ is due, in part, to the dependence on λ on the halo temperature. Simplified calculations, though, within a given dissipative model [65, 42] suggest that the spatial variation of the temperature is only important in the central region of the galaxy and even in that region can (typically) be relatively modest for small galaxies. For the purposes of the analysis given here we shall consider λ in Eq.(4) to be spatially independent as a zeroth order approximation. Under this approximation the spatial dependence of $\rho(r, \theta, \phi)$, Eq.(4), is determined solely by that of the flux, $F_{\gamma_D}(r, \theta, \phi)$.

Eq.(4) is subject to another significant caveat. It provides the mass density only of the diffuse dark matter (plasma) component. Dissipative dark matter models can also have dark matter in the form of ‘dark stars’, that is, stars composed of dark matter particles. Naturally it is quite challenging to figure out the proportion and distribution of such a component, and for the present discussion it will be assumed negligible. ⁴

With the above important qualifications, Eq.(4) provides a description of the dark matter density in a given galaxy. Disk galaxies though come in various sizes, how does λ depend on the galaxy scale? The physical quantity of most interest is again the halo temperature, T . Assuming that the halo is isothermal and in approximate hydrostatic equilibrium, the temperature can be expressed in terms of the maximum value of the rotational velocity: [39, 41, 42]

$$T = \frac{1}{2} \bar{m} [v_{rot}^{max}]^2 \quad (5)$$

where $\bar{m} = \sum n_i m_i / \sum n_i$ is the mean mass of the particles making up the dark plasma. The maximum value of the rotational velocity, v_{rot}^{max} , varies between around 20 km/s for the smallest dwarfs to around 300 km/s for the largest spirals. If we assume that the heating is due to photoionization of K-shell dark atomic states and that the binding energy of these states is larger than the halo temperature of the largest spirals, then the heating rate is approximately independent of the halo’s temperature. The dark photons heating the halo encounter fully occupied K-shell states for all galaxy scales of interest. Cooling, on the other hand, is expected to depend more strongly on the halo’s temperature since the bremsstrahlung cross section depends on temperature, leading to: $\Gamma_{cool} \propto \sqrt{T} n(\mathbf{r})^2$. Thus, these simplified dissipative models suggest that $\lambda \propto 1/\sqrt{T}$, and via Eq.(5) give $\lambda \propto 1/v_{rot}^{max}$. However more complicated behaviour is certainly possible, and would be expected for temperature regions where other cooling processes become important, ⁵ the

⁴Note though that for elliptical galaxies (and possibly dwarf spheroidals) the situation is expected to be very different. For these galaxy types there is (currently) very low star formation rate and therefore heating of the dark halo from ordinary supernovae is not expected to be significant. Any diffuse dissipative dark matter halo around these kinds of galaxies would therefore have collapsed into ‘dark stars’ [42, 41].

⁵For an important class of dissipative models, including those studied in [39, 64, 65, 66, 42, 41], dark atom recombination and line emission can potentially significantly contribute to cooling. These processes also feature $\Gamma_{cool} \propto n(\mathbf{r})^2$ and thus Eq.(4) still holds, but the proportionality constant can have a more complicated dependence on halo temperature. If such processes are dynamically important they can modify the predicted $\lambda(T) \propto 1/\sqrt{T}$ scaling.

details will of course depend on the particle physics properties of the specific dissipative model. As will be discussed in more detail in section 3, this galaxy scaling relation is related to the Tully-Fisher relation [33].

The halo dark matter contribution to the gravitational acceleration at a point in the plane of the disk can be straightforwardly calculated given the density profile, Eq.(4), and Newton's law of gravity. Assuming an azimuthally symmetric disk, the motion of the gas and stars in the disk is circular with speed v_{halo} given by:

$$\frac{v_{halo}^2}{r} = G_N \int d\tilde{\phi} \int d\cos\tilde{\theta} \int d\tilde{r} \tilde{r}^2 \frac{\rho(\tilde{r}, \tilde{\theta}) \cos\omega}{d^2}. \quad (6)$$

Here, $d^2 \equiv r^2 + \tilde{r}^2 - 2r\tilde{r}\sin\tilde{\theta}\cos\tilde{\phi}$, $\cos\omega \equiv (r - \tilde{r}\sin\tilde{\theta}\cos\tilde{\phi})/d$ and G_N is Newton's constant.

In the previous paper [56] the density profile, Eq.(4), was examined by first modelling the supernovae rate with an exponential disk: $\Sigma_{SN}(r) = (R_{SN}/2\pi r_D^2) e^{-r/r_D}$ [68]. This could only be a very crude approximation, since the exponential disk is an approximate measure of the stellar population, including middle aged and older stars, while the quantity we require is the recent (large) star formation rate. Anyway, if $\Sigma_{SN}(r)$ is an exponential function of radius then Eq.(4) becomes roughly equivalent (as far as rotation curves are concerned) to the cored distribution: $\rho_{ISO}(r) = \rho_0 r_0^2 / (r^2 + r_0^2)$, with $r_0 \approx r_D$. Such a constrained quasi-isothermal profile is known to be phenomenologically successful in explaining the observed shapes of rotation curves, e.g. [15, 69, 70, 71, 30, 19]. Dissipative dark matter therefore provides an underlying theoretical explanation for the successful quasi-isothermal profile.

The dark matter density profile of Eq.(4) is, in fact, further constrained. At small radii, $r < r_D$, the dark matter density [Eq.(4)] can be related to the central surface density, $\Sigma_{SN}(0) \equiv R_{SN}/(2\pi r_D^2)$, via:

$$\rho(r) = \frac{\lambda \Sigma_{SN}(0)}{2} \left[\log\left(\frac{r_D}{r}\right) + \text{constant} \right]. \quad (7)$$

This implies a scaling relation connecting the inner circular velocity gradient with this central surface density: $v \propto r \sqrt{\lambda \Sigma_{SN}(0)}$. To connect with measurable quantities, one could replace $\Sigma_{SN}(0)$ with the central surface brightness in the UV band, $\Sigma_{UV}(0)$ and neglect the variation of λ (which is anticipated to be fairly weak for dwarf irregular galaxies). This leads to the rough scaling relation: $v \propto r \sqrt{\Sigma_{UV}(0)}$ or

$$\log\left(\frac{dv}{dr}\right) = -0.2\mu_0 + \text{constant} \quad (8)$$

where μ_0 is the central surface brightness in magnitude units. Such a scaling relation has in fact been observed to hold for spiral and irregular galaxies [32].

In addition to modelling Σ_{SN} via an exponential disk, the previous paper [56] further considered modelling Σ_{SN} in terms of the baryonic gas density via a Kennicutt-Schmidt type relation [57, 58]. This allowed a connection between the supernovae distribution with current local properties of a given galaxy. In the following we shall consider a more direct estimate of the supernovae distribution, by modelling the supernovae distribution via the measured UV and $H\alpha$ fluxes.

3 Dissipative dark matter versus dwarf galaxies

3.1 The LITTLE THINGS dwarfs

In this paper we shall examine all 26 dwarf galaxies comprising the LITTLE THINGS sample [19]. An inspection of these 26 galaxies suggests a loose classification: 18 dwarfs which feature ‘classically’ shaped rotation curves with a (typically) linear rise in v_{rot} near $r = 0$ smoothly transiting to a flat rotation curve at the greatest measured radii, three dwarfs which show a classically shaped rotation curve for r less than some radius, R^* , but show a downturn for $r > R^*$, and four dwarfs which show a classically shaped rotation curve for r less than some radius, R_1 , but feature a ‘hump’ at $r > R_1$. In addition there is one dwarf (DDO47) whose rotation curve is irregularly shaped. In figure 1 we give an example for each of these galaxy types.

The theoretically predicted rotation velocity, v_{rot} , is the sum of the various contributions added in quadrature:

$$v_{rot} = \sqrt{v_{halo}^2 + v_{gas}^2 + v_{stars}^2} . \tag{9}$$

Here, v_{gas} and v_{stars} are the baryonic gas and stellar contributions while v_{halo} is the dark matter contribution, Eq.(6). The latter is given in terms of the density, Eq.(4), which can be evaluated if the supernovae distribution of the galaxy is known. To proceed we therefore need to model the supernovae rate, $\Sigma_{SN}(r)$.

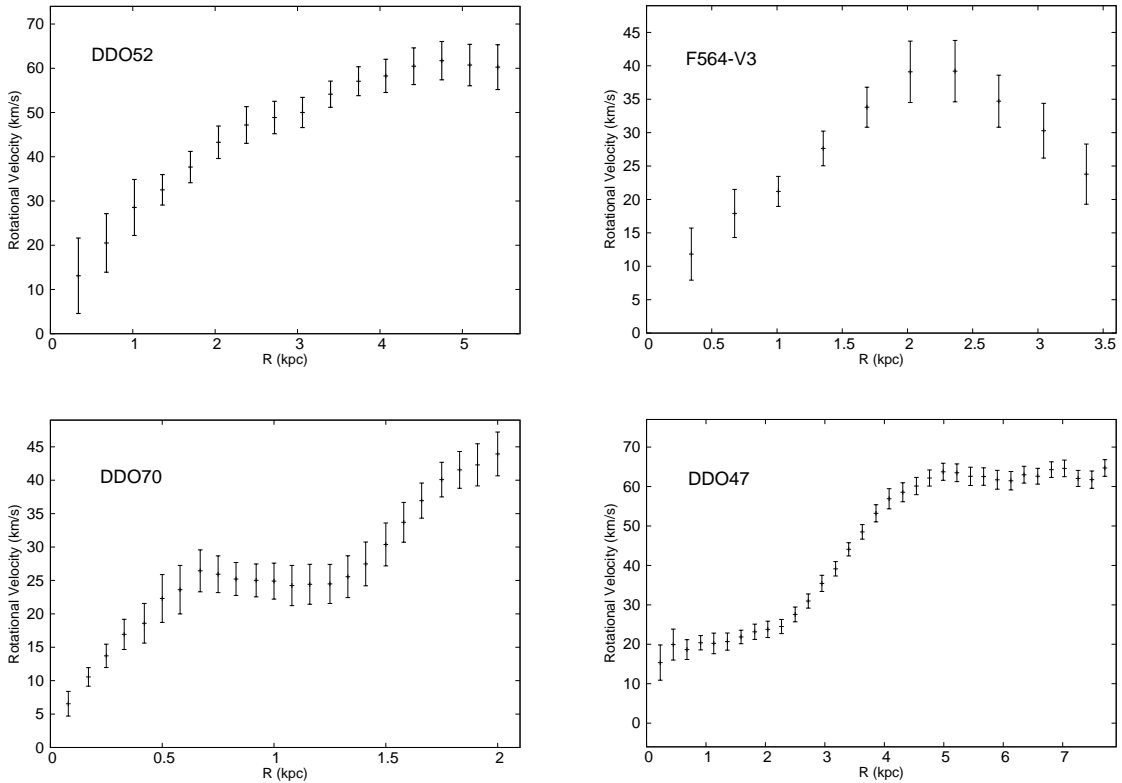


Figure 1: Examples of the four classes of galaxies in the LITTLE THINGS sample: DDO52, classically shaped rotation curve (linear rise, transiting to flat), F564-V3, classically shaped but with a downturn in v_{rot} , DDO70, classically shaped but with a ‘hump’ at large R , DDO47, an irregularly shaped rotation curve.

In the literature UV and $H\alpha$ emission have both been used as traces for star formation rates, see e.g. [72, 73, 74]. The UV radiation is directly emitted from the photospheres of large stars, with $M_* \gtrsim 3M_\odot$ (O- through later-type B-stars) while the $H\alpha$ nebular emission results from the recombination of hydrogen which can only be ionized by very large stars, with $M_* \gtrsim 17M_\odot$ (the most massive O- and early- type B-stars). The $H\alpha$ flux provides a measure of star formation rate on fairly short timescales of ~ 10 Myr, while UV flux provides a measure on a somewhat larger timescales: ~ 100 Myr. The timescale most relevant for the supernovae rate, Σ_{SN} , in Eq.(4) is some appropriately weighted average over the timescale characteristic of the dissipative dynamics, $\tau \sim (3/2)n(r)T/\Gamma_{cool}$, expected to be less than around a Gyr as mentioned earlier. A priori, both UV and $H\alpha$ fluxes present reasonable candidates for the relevant supernovae rate, and we will consider both profiles in the χ^2 analysis to follow.

The Galaxy Evolution Explorer (GALEX) [75] has obtained images of nearby galaxies in the far UV (FUV) bandpass of 1350-1750 Å and near UV (NUV) bandpass of 1750-2800 Å. The GALEX data was analyzed in [76] for a large selection of dwarf galaxies, including 24 of the LITTLE THINGS sample of 26 galaxies, yielding the azimuthally averaged surface brightnesses, $\mu_{FUV}(r)$. This quantity can be converted to the flux density via the standard formula: $F_{FUV}(r) = 10^{-0.4(\mu_{FUV}(r)+48.6)}$ erg cm⁻² s⁻¹ Hz⁻¹ arcsec⁻², and similarly for the NUV flux. Also given in that reference is the $H\alpha$ surface brightnesses, $\mu_{H\alpha}$, which can also be converted to a $F_{H\alpha}(r)$ flux. In the following, we shall model $\Sigma_{SN}(r)$ with each of these fluxes. Of most interest is the radial dependence of these quantities as the overall proportionality constant can be absorbed into a redefinition of the coefficient λ of Eq.(4); this redefinition is denoted as $\tilde{\lambda}$ (and will be defined more precisely later on).

Consider first the 18 classical dwarfs and DDO47. In table 1 we give some properties of these galaxies: the distance of the galaxy as given in [19] and also the absolute AB FUV-band magnitude (evaluated from the apparent magnitude assuming this distance measurement).⁶ Also given in table 1 is $\chi_r^2 = \chi^2/N_{dof}$ (for a 1 parameter fit, the number of degrees of freedom is $N_{dof} = N_{data} - 1$) for the fit of the model to the rotation curve data, modelling $\Sigma_{SN}(r)$ with a) $F_{FUV}(r)$, b) $F_{NUV}(r)$ and c) $F_{H\alpha}$, each obtained from [76] as described above.⁷ Here, the χ^2 function for each galaxy is constructed in the usual way:

$$\chi^2 \equiv \sum_{i=1}^{N_{data}} \left[\frac{v_{rot}(i) - v_{rot}^{exp}(i)}{\delta v_{rot}^{exp}(i)} \right]^2 \quad (10)$$

where the N_{data} (asymmetric drift corrected) binned rotation curve measurements, $v_{rot}^{exp}(i) \pm \delta v_{rot}^{exp}(i)$, are obtained from [19] and v_{rot} is evaluated via Eq.(9) (with v_{gas} and v_{stars} from [19]). This χ^2 function was minimized with respect to variations of the parameter λ (which was allowed to have a different value for each galaxy). The related quantity, $\tilde{\lambda}$, to be defined in Eq.(14), is also given in the table.

The χ^2 values given in the table suggests that the density profile, Eq.(4), motivated by the dissipative dynamics is consistent with a zeroth order approximation for most of the 18 classical dwarfs. The resulting fits are shown in figures 2-4 for the 18 ‘classical’ dwarfs and DDO47. In these figures, the FUV flux was used as the tracer for Σ_{SN} ;

⁶For dwarf galaxies extinction corrections are generally small. For the estimated FUV absolute magnitude of the dwarf galaxies the internal and galactic (foreground) extinction corrections were nevertheless included following the procedure of [74, 73] using data obtained by the online updated nearby galaxy catalogue [77].

⁷For the dwarfs: DDO52, DDO101, DDO210, DDO216. there were insufficient $H\alpha$ flux measurements for which to construct the flux, while for IC10 UV flux measurements were unavailable.

very similar results occur for the other two traces considered. Indeed, as the χ_r^2 values in the table indicate, use of the NUV flux generally leads to a slightly better fit to the rotation curve data, while with the $H\alpha$ flux the fit fares slightly worse. It is also noted that use of UV flux generally leads to a slightly better fit to the rotation curves than the Kennicutt-Schmidt-type power law considered in [56].⁸

The density profile, Eq.(4), is highly constrained as it depends on just one parameter λ . This parameter sets the normalization of the dark halo contribution of the rotation curve. The shape of the curve is fully predicted by Eq.(4) once the supernovae distribution is input via the FUV flux radial profile. Figures 2-4 indicate that the radius where the rotation curve transitions from linear to flat is generally reproduced reasonably well.⁹ Note though that the rotation curve error bars are not purely statistical as they are usually derived by taking the difference between rotation curve measurements from each side of the galaxy. It is possible that the small but perceptible difference between the fit and the data of some of these galaxies is an indication for corrections to the zeroth order approximation of Eq.(4). There are many possible sources of corrections including: radial dependence of the halo temperature, modelling of the supernova distribution, correcting for azimuthal asymmetry etc. A simple way to incorporate first order corrections is to allow λ in Eq.(4) to be spatially dependent: $\lambda(r) = \lambda_0 + \lambda_1 r + \dots$. Keeping only the first two terms gives a dark matter density defined in terms of two parameters, λ_0 , λ_1 . The two parameter fit for two examples, DDO154 and WLM is shown in figure 5. As this figure illustrates, the inclusion of first order corrections in this simple phenomenological manner allows for an improved representation of the data.

We now consider the three dwarfs with a downturn in v_{rot} . A possible explanation for the downturn is that it represents the physical extent of the dark halo for these galaxies. If this is the case then we could try to model this boundary effect with a sharp cut-off:

$$\begin{aligned}\lambda(r) &= \lambda \text{ for } r \leq R^*, \\ \lambda(r) &= 0 \text{ for } r > R^* .\end{aligned}\tag{11}$$

This introduces one additional parameter, R^* . The χ_r^2 values for this two parameter (λ , R^*) fit are given in table 2 and the resulting fits are shown in figure 6. It is of course also possible that the downturn is an indication that the halos of these dwarfs are not currently in a steady-state configuration due to some perturbation. This is also a possible explanation of the dwarfs with a ‘hump’, as we will now examine.

The four remaining dwarfs of the LITTLE THINGS sample are those which feature a ‘hump’ at the boundary region. The hump feature might be taken as an indication that the halos of these dwarfs are not entirely in a steady-state configuration where heating and cooling rates locally balance. This situation could conceivably arise if a galaxy was being perturbed, either externally by a nearby galaxy or via some internal mechanism. Such perturbations, if significant, would affect the star formation rate of the galaxy. This suggests that a galaxy’s recent star formation history could possibly be used as a diagnostic aid in determining whether its dark halo is likely to be in a steady-state configuration.

It may also be possible for a galaxy to be in a partially equilibrated state. Perhaps only the inner part of the halo could be in an approximate steady-state configuration.

⁸A curious exception is DDO47, for which the Kennicutt-Schmidt type power law ($\Sigma_{SN}(r) \propto [\Sigma_{gas}(r)]^N$) leads to a significantly better fit: $\chi_r^2(KS) = 5.2$ (for exponent $N = 2$), $\chi_r^2(KS) = 6.7$ (for exponent $N = 3$) cf. $\chi_r^2(FUV) = 9.7$.

⁹In fact, this reproduction is also insensitive to the uncertainty in the distance of the galaxy, D . This can most easily be seen by working with the angular variable, r/D , and noting that both rotation curves and surface photometry are measured in terms of such a quantity.

Galaxy	D (Mpc)	M_{FUV}	χ_r^2 (FUV)	χ_r^2 (NUV)	χ_r^2 ($H\alpha$)	$\tilde{\lambda}$ (km^2/s^2)
18 classical dwarfs						
DDO43	7.8	-13.14	0.55	0.69	0.72	5.32E-3
DDO50	3.4	-15.42	3.53	3.52	3.06	4.36E-4
DDO52	10.3	-13.36	0.18	0.15	-	1.50E-2
DDO53	3.6	-12.51	1.30	1.25	1.30	4.26E-3
DDO87	7.7	-13.09	0.96	0.79	2.54	1.41E-2
DDO101	6.4	-11.59	28.6	22.9	-	0.11
DDO126	4.9	-13.39	0.56	0.55	0.92	4.62E-3
DDO133	3.5	-13.00	5.1	4.1	6.4	1.22E-2
DDO154	3.7	-13.10	0.81	0.83	0.80	1.01E-2
DDO210	0.9	-8.23	0.84	0.69	-	4.53E-2
DDO216	1.1	-9.48	0.50	0.53	-	2.98E-2
IC10	0.7	-	-	-	0.07	-
NGC1569	3.4	-16.80	0.61	0.61	0.50	9.81E-5
NGC2366	3.4	-15.32	0.28	0.27	0.23	1.90E-3
NGC3738	4.9	-14.72	6.14	4.27	3.32	1.56E-2
WLM	1.0	-12.51	0.53	0.44	0.92	9.29E-3
Haro29	5.9	-13.68	0.40	0.40	0.55	3.71E-3
Haro36	9.3	-14.61	1.86	1.63	1.90	1.72E-3
A dwarf with irregularly shaped rotation curve						
DDO47	5.2	-13.83	9.7	10.8	12.5	9.33E-3

Table 1: LITTE THINGS classical dwarfs (defined in text) and DDO47. D (M_{FUV}) is the distance (FUV absolute AB magnitude) of the dwarf and χ_r^2 given for the 1-parameter (λ) fit of the rotation curve data to the model, Eq.(6), Eq.(4), modelling $\tilde{\Sigma}_{SN}$ with a) FUV, b) NUV and c) $H\alpha$ surface brightness radial profiles. The fitted parameter $\tilde{\lambda}$, Eq.(14), is also given.

Galaxy	D (Mpc)	M_{FUV}	χ_r^2 with R^* (kpc)	$\tilde{\lambda}$ (km^2/s^2)
DDO46	6.1	-13.15	3.85 with $R^* = 1.90$	3.19E-2
DDO168	4.3	-13.64	3.20 with $R^* = 3.07$	9.10E-3
F564-V3	8.7	-10.94	0.56 with $R^* = 2.15$	5.47E-2

Table 2: LITTLE THINGS dwarfs with a downturn in the rotational velocity. D (M_{FUV}) is the distance (FUV absolute AB magnitude) of the dwarf and χ_r^2 is given for the 2-parameter (λ , R^*) fit of the rotation curve data to the model, Eq.(6), Eq.(4), Eq.(11). The supernovae distribution, $\tilde{\Sigma}_{SN}$, is here modelled with the FUV surface brightness radial profile. The fitted parameter $\tilde{\lambda}$, Eq.(14), is also given.

Galaxy	D (Mpc)	M_{FUV}	χ_r^2 (FUV) for $r < R_1$ (kpc)	$\tilde{\lambda}$ (km^2/s^2)
CVn1dwA	3.6	-11.56	1.24 for $r < 1.4$	1.41E-3
DDO70	1.3	-11.92	0.71 for $r < 1.6$	1.19E-2
IC1613	0.7	-12.80	1.15 for $0.3 < r < 1.7$	2.38E-4
UGC8508	2.6	-	1.72 for $r < 1.4$	-

Table 3: LITTLE THINGS dwarfs with a ‘hump’ in the rotational velocity. D (M_{FUV}) is the distance (FUV absolute AB magnitude) and χ_r^2 is given for the 1-parameter (λ) fit of the rotation curve data to the model, Eq.(6), Eq.(4), for the inner radial region, $r < R_1$. The supernovae distribution, Σ_{SN} , is here modelled with the FUV surface brightness radial profile, except for UGC8508 which was modelled with $H\alpha$ (FUV was unavailable in the case). The fitted parameter $\tilde{\lambda}$, Eq.(14), is also given.

This situation might arise because of the disparate timescales: the higher density inner region of a dark halo can cool and equilibrate more rapidly than the less dense outer region. The dwarfs with a ‘hump’ (and possibly also those with a ‘bump’) might result from such a condition. In table 3 and figure 7 we show the results of the fit to the inner region of the dwarfs with a ‘hump’.

It is perhaps noteworthy that some of the dwarfs which feature poor fits to the steady-state solution, Eq.(4), are known to be undergoing starburst activity. In particular, of the four dwarfs with the lowest λ values, DDO50, NGC1569, IC1613 and CVn1dwA, three of them [NGC1569, DDO50 (Holmberg II) and CVn1dwA (UGCA292)] are known to be in a starburst phase, e.g. [74, 78]. In fact, a low value of λ is an indication that halo heating exceeds cooling ($\Gamma_{heat} > \Gamma_{cool}$) a situation which would imply that these halos are currently expanding.

Dissipative dynamical halos of the type envisaged here would be expected to play an important role in regulating the star formation rate of a given galaxy. Any perturbation either external or internal that causes the halo to move out of equilibrium, $\Gamma_{heat} \neq \Gamma_{cool}$, would lead to an expanding or contracting halo dynamically adjusting under the various forces. Such dynamics, which could in principle be described by Euler’s equations of fluid dynamics, would be expected to be a major influence on ordinary star formation rates. As the halo expands or contracts, the baryonic gas density decreases or increases in response to the changing gravity. These physical changes in baryonic gas density would in turn correlate with the star formation rate (as suggested by the Kennicutt-Schmidt relation). This interplay between the dynamical halo and star formation rates could be one of the main drivers of starburst activity. It is a temporary non-equilibrium phase where $\Gamma_{cool} \neq \Gamma_{heat}$ and the halo is undergoing significant changes influencing the star formation rate and indeed vice versa.

The dwarf DDO101 has the distinction of featuring the worst fit, with $\chi_r^2(FUV) = 28.6$. It was emphasised in [19] that the inner slope of DDO101 does have potentially large uncertainty due to possible beam smearing effects. Whether such effects could reconcile the predicted rotation curve with the data is unclear. If this (or other) systematic effects are not responsible for the disagreement, then one could speculate that this very faint dwarf has evolved to the point where there is insufficient heating to support the halo. The halo may have cooled and collapsed (or is in the process of collapsing) into dark stars. Indeed table 1 indicates that the λ value for this dwarf is anomalously large, which is evidence in favour of this interpretation.

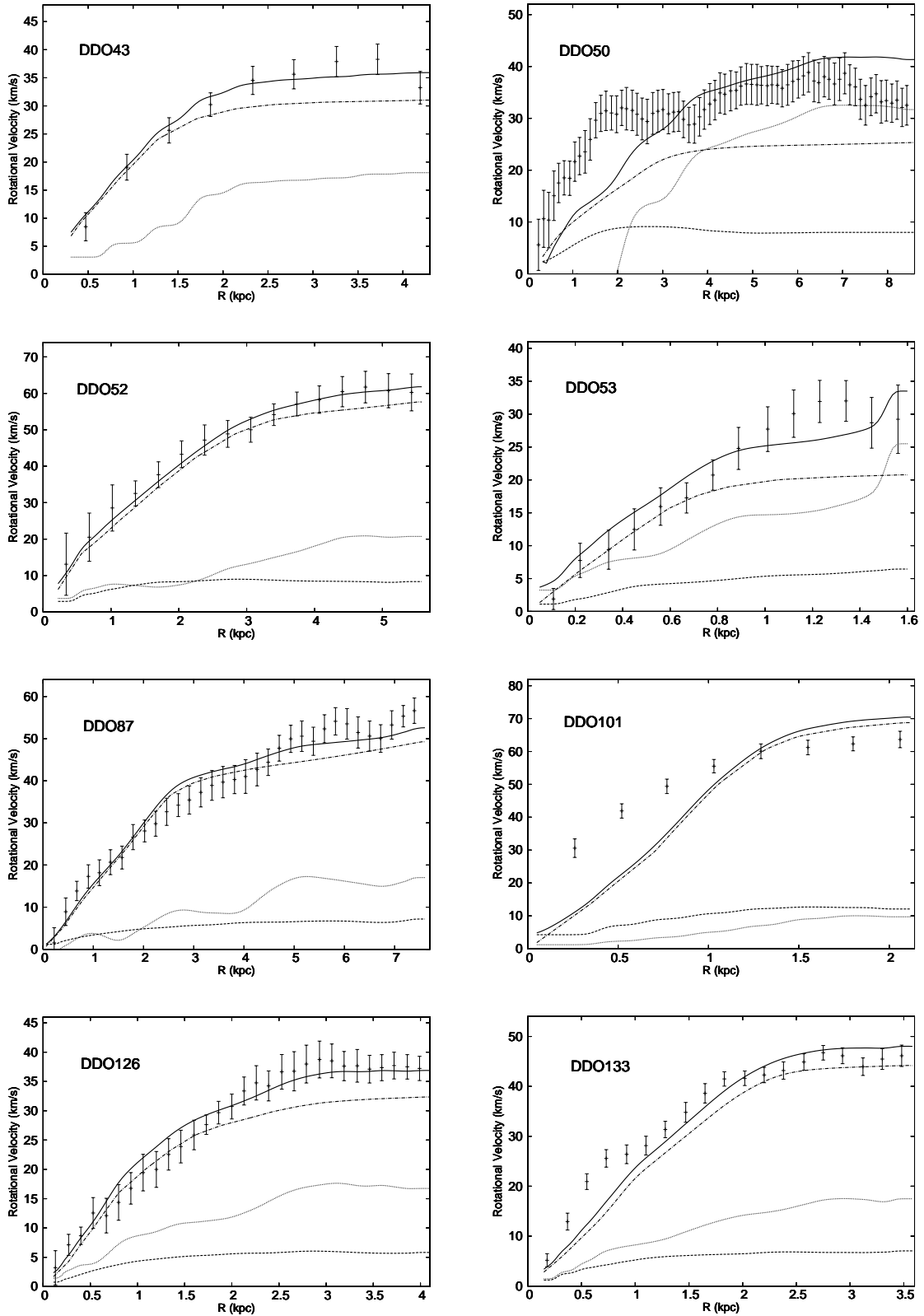


Figure 2: Rotation curves for the dwarf galaxies, DDO43, DDO50, DDO52, DDO53, DDO87, DDO101, DDO126 and DDO133. The data is from [19]. The stellar (dashed line), baryonic gas (dotted line) and dissipative dark halo (dashed dotted line) contributions are shown. The solid line is the sum of these contributions added in quadrature. The halo contribution results from the 1-parameter fit, Eq.(4) with λ assumed spatially independent. $[\Sigma_{SN}$ in Eq.(4) is modelled via the FUV surface brightness radial profile from [76] as described in the text.]

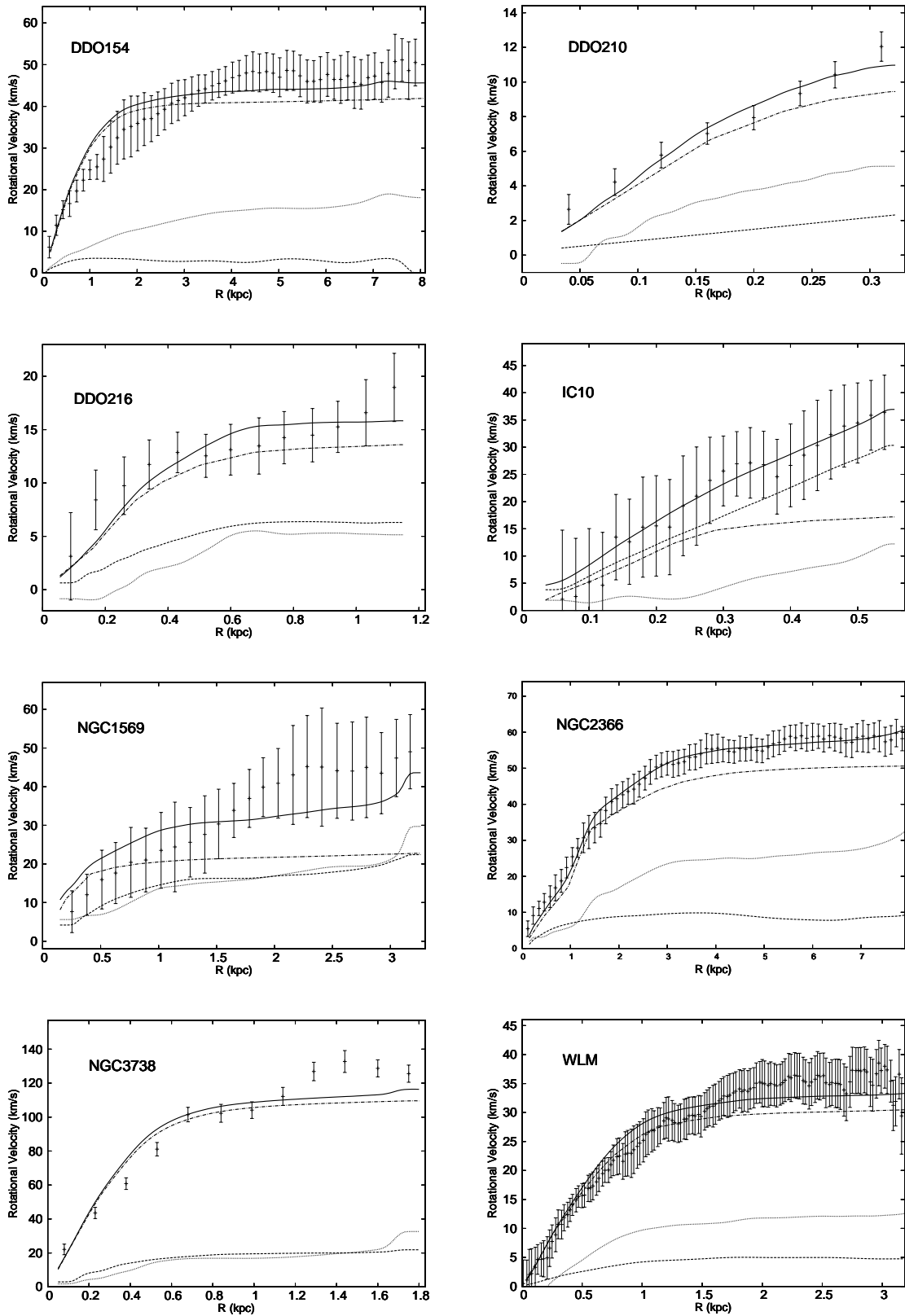


Figure 3: Rotation curves for the dwarf galaxies, DDO154, DDO210, DDO216, IC10, NGC1569, NGC2366, NGC3738 and WLM. Notation as in figure 2.

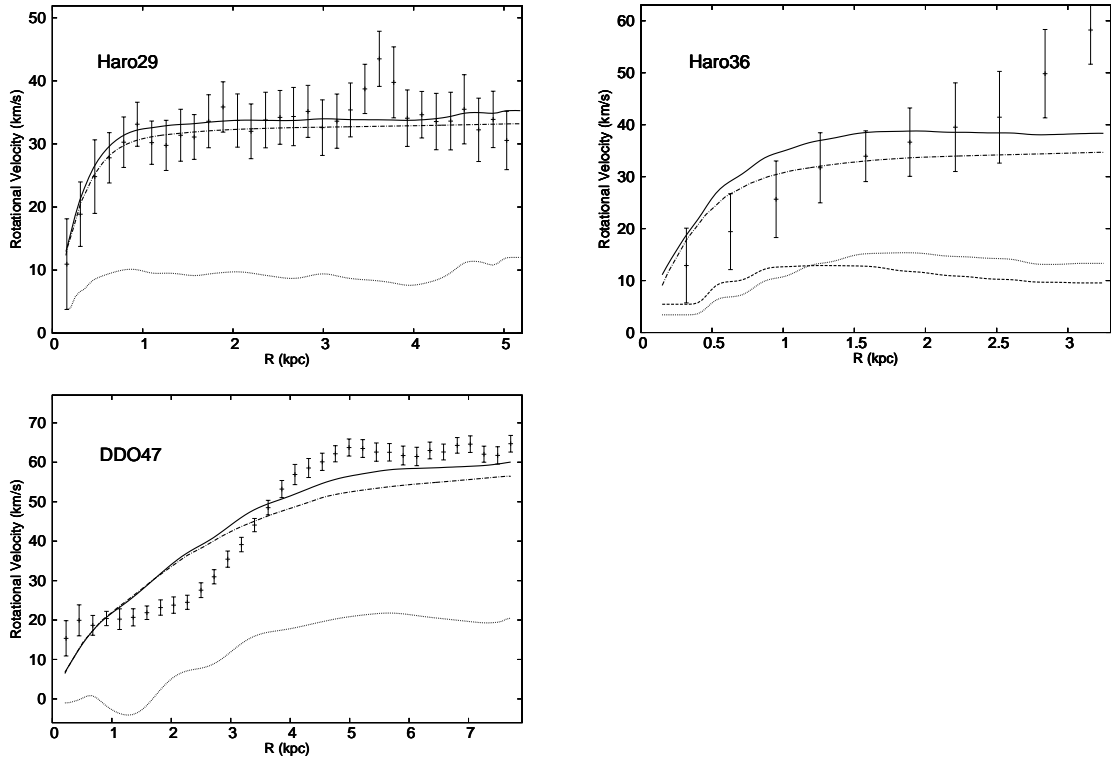


Figure 4: Rotation curves for the remaining two ‘classically’ shaped dwarfs: Haro29 and Haro 36 and also the irregularly shaped rotation curve of DDO47. Notation as in figure 2.

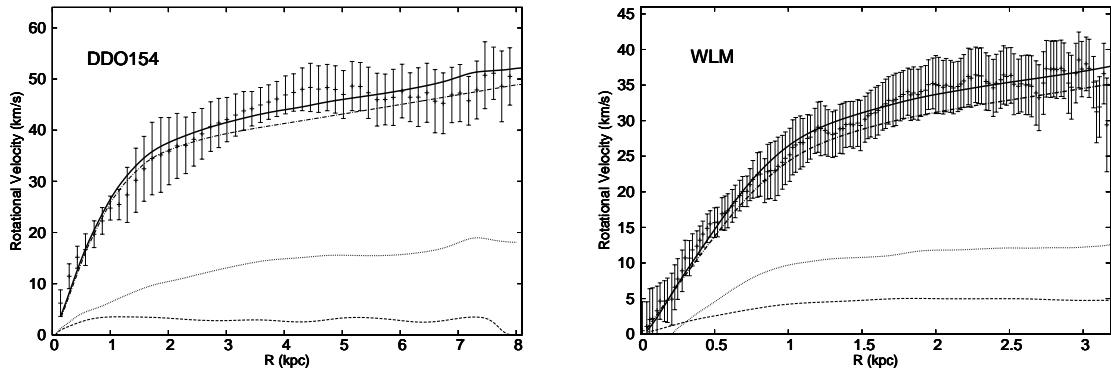


Figure 5: Rotation curves for DDO154 and WLM. Notation as in figure 2, except that the halo contribution was calculated from Eq.(4) allowing for a spatially dependent λ : $\lambda(r) = \lambda_0 + \lambda_1 r$ and thus a two-parameter fit.

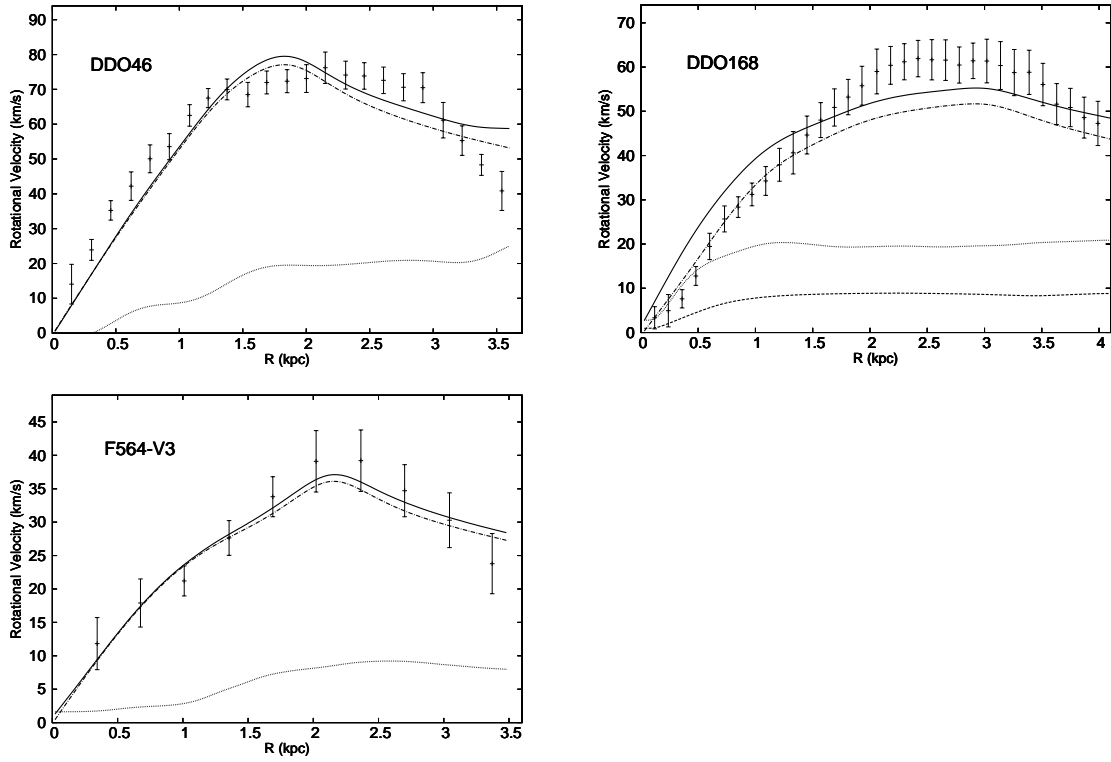


Figure 6: Rotation curves for the three dwarf galaxies, DDO46, DDO168, F564-V3, indicating a downturn in v_{rot} . The downturn is modelled with a hardcut off in the dark matter density, as described in the text. Notation as in figure 2.

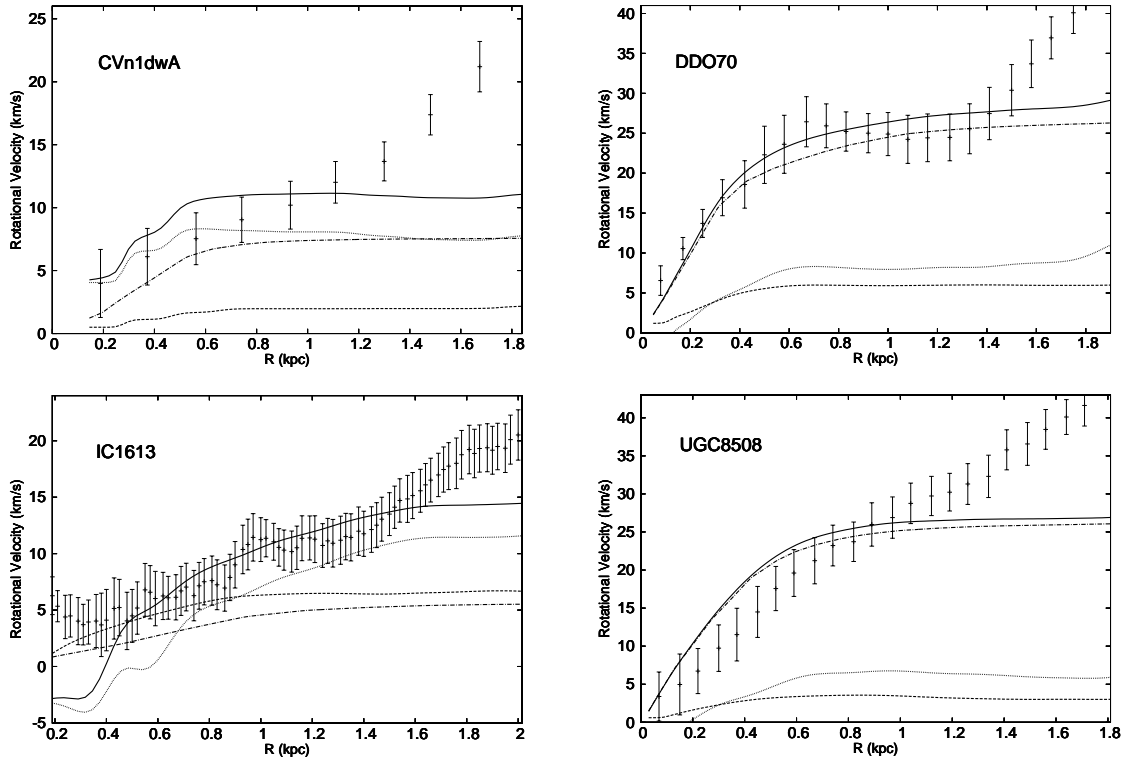


Figure 7: Rotation curves for the remaining LITTLE THINGS dwarfs [CVn1dwA, DDO70, IC1613, UGC8508] which feature a ‘hump’ at the largest measured radii. Shown are fits to the inner part of the rotation curve data, see discussion in text. Notation as in figure 2.

Galaxy	D (Mpc)	M_{FUV}	$\tilde{\lambda}$ (km ² /s ²)
NGC925	9.2	-18.28	6.1E-4
NGC2403	3.2	-17.85	1.2E-3
NGC2841	14.1	-18.77	2.0E-3
NGC2903	8.9	-18.45	1.2E-3
NGC2976	3.6	-14.67	6.6E-3
NGC3031	3.6	-18.08	4.8E-4
NGC3198	13.8	-18.97	4.4E-4
NGC3521	10.7	-18.37	1.5E-3
NGC3621	6.6	-18.29	8.8E-4
NGC4736	4.7	-16.86	6.5E-4
NGC5055	10.1	-18.57	9.4E-4
NGC6946	5.9	-18.74	8.4E-4
NGC7331	14.7	-18.96	7.5E-4
NGC7793	3.9	-17.18	1.5E-3

Table 4: THINGS spirals: D is the distance of the spiral and M_{FUV} is the FUV absolute AB magnitude corrected for internal and foreground extinction. Also given is the parameter $\tilde{\lambda}$, Eq.(14).

3.2 THINGS spirals

Let us now briefly comment on spiral galaxies. Compared to dwarf irregular galaxies, spirals have a much larger stellar component, which typically dominates over the dark matter contribution in the inner part of the galaxy. This stellar component is poorly constrained due to uncertain stellar mass-to-light ratio, Υ_* . This unfortunately tends to make spirals much less useful in testing dark matter models. Also, the UV and $H\alpha$ flux measurements for spirals have larger uncertainties due to much larger extinction corrections. A sample of spirals with high resolution rotation curves has been given by the THINGS collaboration [59]. An example is given in figure 8, where the fit to the rotation curve of NGC2403 is given. In this example the baryonic contribution was obtained from [59] and modelled allowing Υ_* to vary, and the dark matter contribution was obtained from Eq.(6) and Eq.(4). The supernovae rate in Eq.(4) was modelled via a Kennicutt-Schmidt relation, with exponent $N = 2$, $\Sigma_{SN} \propto \Sigma_{gas}^2$ (UV surface profile was unavailable).

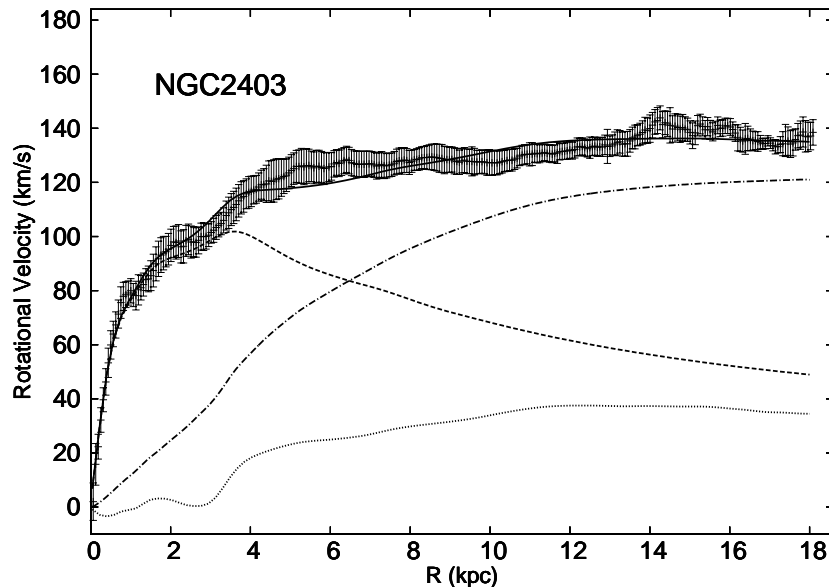


Figure 8: The spiral galaxy, NGC2403. The stellar (dashed line), baryonic gas (dotted line) and dissipative dark halo (dashed dotted line) contributions are shown. The solid line is the sum of these contributions added in quadrature.

3.3 The scaling of λ

In the fits of the dwarf galaxies the parameter λ in Eq.(4) was allowed to have a different value for each galaxy. In specific dissipative dark matter models this parameter is expected to have a more universal character, with simple arguments suggesting a weak scaling: $\lambda \propto 1/v_{rot}^{max}$ [see earlier discussion around Eq.(5)].

At sufficiently large radii the dark photon flux falls at the geometric rate: $F_{\gamma_D} \propto 1/r^2$. At such large radii the dark matter halo mass density profile [Eq.(4)] reduces to:

$$\rho(r) = \lambda \frac{R_{SN}}{4\pi r^2}. \quad (12)$$

Here R_{SN} is the integrated supernova rate in the disk. Eq.(6) gives an asymptotically flat value for the halo contribution to the circular velocity:

$$v_{halo}^2 = \lambda G_N R_{SN}. \quad (13)$$

Supernovae are the final evolutionary stage of large stars. As discussed earlier, the FUV luminosity (L_{FUV}) is expected to provide a reasonably direct estimate of the star formation rate, so that: $R_{SN} \propto L_{FUV} \propto 10^{-0.4M_{FUV}}$. It is convenient then to introduce the quantity $\tilde{\lambda}$:

$$\tilde{\lambda} \equiv \frac{v_{halo}^2}{10^{-0.4M_{FUV}}}. \quad (14)$$

With this definition Eq.(13) implies $\tilde{\lambda} = \lambda G_N c_1$ where $c_1 \equiv R_{SN}/10^{-0.4M_{FUV}}$. For each galaxy, v_{halo} can be obtained from the fit of the model to the rotation curve data (for the dwarfs with a downturn in v_{rot} , listed in table 2, we set $v_{halo} = v_{rot}^{max}$). The absolute FUV AB magnitude, M_{FUV} , has already been provided in tables 1-3 for the 24 dwarfs for which FUV flux measurements are available. These tables also give the resulting $\tilde{\lambda}$

values, as defined in Eq.(14), for each dwarf. We have also estimated the $\tilde{\lambda}$ values for the THINGS spirals. For these spirals we obtained v_{halo} from the quasi-isothermal fit with free mass-to-light stellar mass parameter as given in [59]. The absolute FUV magnitude was obtained using data from [77, 79] and corrected for both internal and foreground extinction following the procedure of [74, 73]. The results of this exercise are given in table 4. Figure 9 summarizes these results.¹⁰

Under the assumptions that the halo heating is approximately independent of the halo temperature, T , and halo cooling is dominated by bremsstrahlung, $\Gamma_{cool} \propto \sqrt{T}n^2$, one expects the rough scaling $\lambda \propto 1/\sqrt{T}$. As discussed earlier in section 2 [see discussion around Eq.(5)], this leads to the correlation: $\lambda \propto 1/v_{rot}^{max}$. Assuming that c_1 (defined above) is constant this then implies $\tilde{\lambda} \propto 1/v_{rot}^{max}$ or equivalently,

$$L_{FUV} \propto v_{halo}^2 v_{rot}^{max} . \quad (15)$$

This scaling is also shown in figure 9. For many galaxies one could make the rough approximation: $v_{halo} \approx v_{rot}^{max}$, from which Eq.(15) reduces to: $L_{FUV} \propto [v_{rot}^{max}]^3$. For spiral galaxies, this is approximately equivalent to the Tully-Fisher relation [33], e.g. the study [80] found that $L_B \propto [v_{rot}^{max}]^\alpha$, where $\alpha = 3.4 \pm 0.09$ (the difference between this exponent and the value $\alpha = 3$ is consistent with the slight scaling difference between the FUV and B-bands).

Figure 9 shows a significant scatter of the $\tilde{\lambda}$ parameter for the LITTLE THINGS dwarf galaxies. Some scatter can be due to uncertainties, e.g. the determination of the galaxy’s absolute magnitude will be affected by the uncertainty in its distance, the parameter c_1 might vary somewhat between different galaxies etc., however such uncertainties are unlikely to be the whole explanation¹¹. The size of the scatter might indicate fundamental physical differences between galaxies, or it could simply be an indication that the dissipative halos are not all in a steady-state configuration. Halo heating and cooling rates may be unbalanced due to perturbations from nearby galaxies, current (or recent) starburst activity etc. As already discussed, such activity might cause distortions including, possibly, the ‘bump’ and ‘hump’ in the rotation curves apparent in a subset of the dwarfs. If so, then it could be a factor behind the poor fits to the shape of the rotation curve that some of the dwarfs feature. In figure 10 we therefore consider only a subset of galaxies: the THINGS spirals together with the LITTLE THINGS classical dwarfs and only those with $\chi_r^2(FUV) < 2$. This means that the dwarfs DDO101, DDO50, DDO133, NGC3738 (and those of tables 2 and 3) are excluded, and we also exclude NGC1569 which is undergoing extreme starburst activity [78] (whose halo is therefore unlikely to be in an equilibrium configuration).

Figure 10 shows a much reduced scatter (cf. figure 9) of the $\tilde{\lambda}$ values with respect to the $\tilde{\lambda} \propto 1/v_{rot}^{max}$ scaling. This is some evidence in favour of a ‘universal’ λ parameter, presumably set in part by the fundamental particle physics of the dissipative model. Further studies, with a larger sample would be a useful next step. In particular, the possible validity of Eq.(15) over the entire range from dwarfs to spirals warrants further investigation, along with possible connection with the baryonic Tully-Fisher relation [34].

¹⁰The uncertainty in the parameter $\tilde{\lambda}$ was estimated from the distance uncertainty, v_{halo} uncertainty, and the uncertainty in the extinction corrections. The distance uncertainty for most of the galaxies is small, typically 10%, while the v_{halo} uncertainty was taken from the rotation velocity data points at large radii. The uncertainty in extinction was assumed to be $\pm 20\%$ of the extinction correction.

¹¹Note however that since Eq.(4) defines the dark matter density directly in terms of the supernova density (rather than say, baryonic mass), the estimated values for $\tilde{\lambda}$ should be independent of the uncertain mass-to-light ratio of the galaxy.

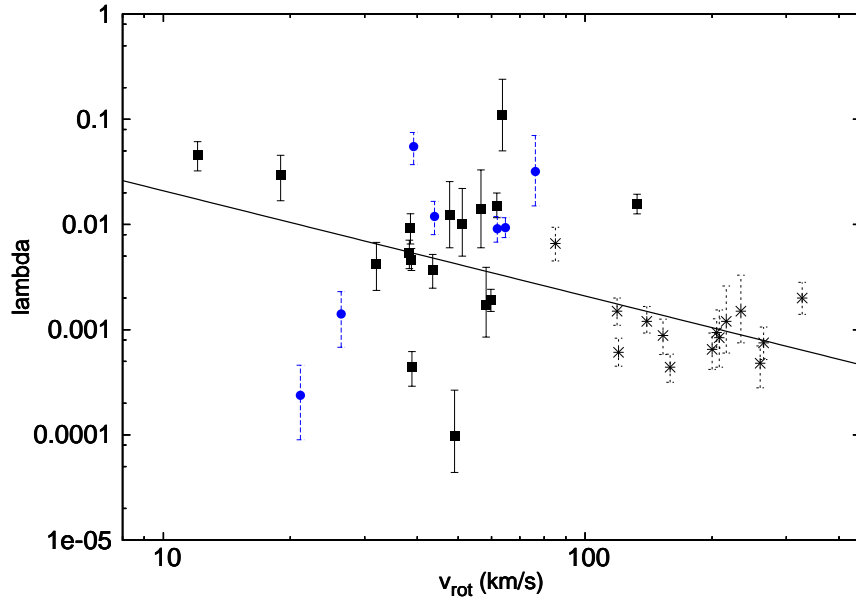


Figure 9: The parameter $\tilde{\lambda}$ [Eq.(14)] versus v_{rot}^{max} for the LITTLE THINGS dwarfs (squares and circles) and THINGS spirals (stars). The squares are the classical dwarfs while the circles are all the others. The solid line is the $\tilde{\lambda} \propto 1/v_{rot}^{max}$ scaling discussed in text.

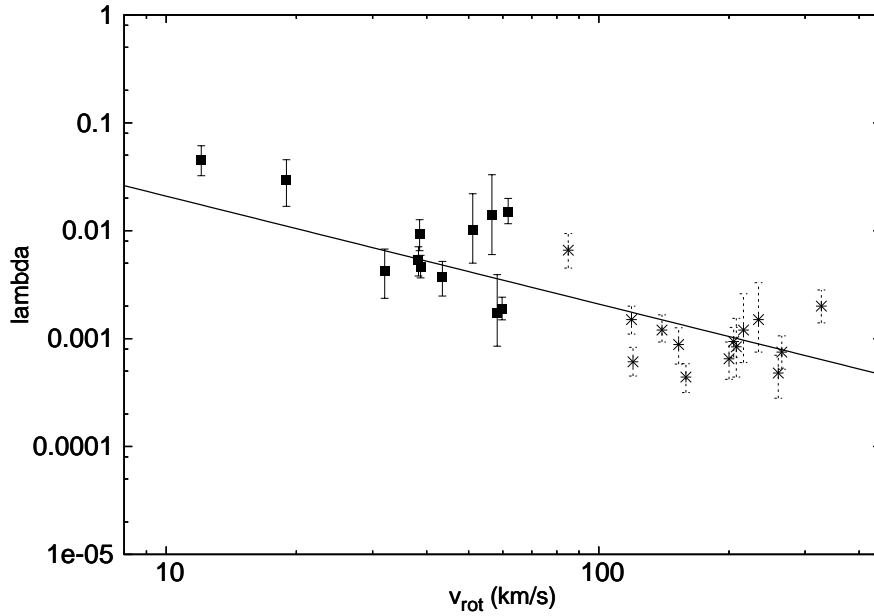


Figure 10: Same as figure 9 except only THINGS spirals and ‘best fit’ classical dwarfs are included (see text).

4 Conclusion

There is substantial evidence from rotation curves that dark matter halos have nontrivial dynamics. Most striking is that the observed rotation curves are strongly correlated with the baryon content. The Tully-Fisher relation provides a global relation, while the dark matter rotational velocity generally transits from linear rise (near the galactic center) to flat at a distance scale associated with the baryonic distribution, and there are also many other correlations.

Dark matter halos around disk galaxies can have such nontrivial dynamics if dark matter is strongly self interacting and dissipative. Multicomponent hidden sector dark matter featuring a massless ‘dark photon’ (from an unbroken dark $U(1)$ gauge interaction) which kinetically mixes with the ordinary photon provides a concrete example of such dark matter. The kinetic mixing interaction facilitates halo heating by enabling ordinary supernovae to be a source of these dark photons. Dark matter halos can expand and contract in response to the heating and cooling processes, but for a sufficiently isolated and unperturbed halo should have evolved to a steady state or ‘equilibrium’ configuration where heating and cooling rates locally balance. This dynamics allows the current dark matter density profile to be related to the distribution of ordinary supernovae in the disk of a given galaxy, Eq.(4). Naturally, this is a simplified description and would likely be invalid for galaxies strongly influenced by perturbations, starburst activity etc.

The ordinary supernovae distribution was here modelled via the UV light emission profile, which should provide a fairly direct measurement of this distribution in a given galaxy. This improves upon previous work of [56] which used the gas density via a Kennicutt-Schmidt type relation. The resulting halo rotation curve then depends on only one parameter λ (assumed to be spatially independent as a zeroth order approximation) and tested against the full LITTLE THINGS sample of 26 dwarf galaxies. The analysis indicates that for most of the LITTLE THINGS dwarfs, the dark matter predictions resulting from the simple formula, Eq.(4), agree reasonably well with the observations. Not all of the dwarfs analysed have good agreement, however the poor fits of some of these dwarfs can plausibly be ascribed to environmental influences which perturb the halo. Such a perturbation may only be temporary, the timescale depending on the nature of the perturbation and the details of the dissipative particle physics.

In the simplified approach considered here, the steady-state configuration, Eq.(4), is described by a single parameter, λ . This parameter is a function of various fundamental parameters, e.g. in the model of [41] one has dark particle masses, dark fine structure constant etc. The parameter λ also depends on less fundamental parameters, including galaxy-dependent quantities such as halo temperature. Although in principle λ can be a complicated function of these parameters, some simple arguments favour an approximate scaling with the halo temperature, $\lambda \propto 1/\sqrt{T}$. Such a simple scaling is roughly consistent with the analysis of the LITTLE THINGS dwarfs and THINGS spirals presented here. Deviations from this scaling are possible and can in principle be calculated within a given dissipative particle model, and could thereby provide an important means of testing and constraining the underlying particle physics.

Acknowledgments

The author would like to thank: S. Oh and W. de Blok for making available rotation curve data files. The author would also like to thank S. Oh and also I. D. Karachentsev for some helpful correspondence. This work was supported by the Australian Research Council.

References

- [1] P. A. R. Ade *et al.* [Planck Collaboration], *Astron. Astrophys.* **571**, A16 (2014) [arXiv:1303.5076].
- [2] R. Keisler *et al.*, *Astrophys. J.* **743**, 28 (2011) [arXiv:1105.3182].
- [3] G. Hinshaw *et al.* [WMAP Collaboration], *Astrophys. J. Suppl.* **208**, 19 (2013) [arXiv:1212.5226].
- [4] M. Tegmark *et al.* [SDSS Collaboration], *Astrophys. J.* **606**, 702 (2004) [astro-ph/0310725].
- [5] S. Cole *et al.* [2dFGRS Collaboration], *Mon. Not. Roy. Astron. Soc.* **362**, 505 (2005) [astro-ph/0501174].
- [6] C. Blake *et al.*, *Mon. Not. Roy. Astron. Soc.* **418**, 1707 (2011) [arXiv:1108.2635].
- [7] C. P. Ahn *et al.* [SDSS Collaboration], *Astrophys. J. Suppl.* **203**, 21 (2012) [arXiv:1207.7137].
- [8] L. Anderson *et al.*, *Mon. Not. Roy. Astron. Soc.* **427**, 3435 (2013) [arXiv:1203.6594].
- [9] K. S. Dawson *et al.* [BOSS Collaboration], *Astron. J.* **145**, 10 (2013) [arXiv:1208.0022].
- [10] V. C. Rubin and W. K. Ford, Jr., *Astrophys. J.* **159**, 379 (1970).
- [11] M. A. Roberts and A. H. Rots, *Astron. Astrophys.* **26**, 483 (1973).
- [12] V. C. Rubin, N. Thonnard and W. K. Ford, Jr., *Astrophys. J.* **238**, 471 (1980).
- [13] A. Bosma, PhD thesis, University of Groningen (1978); *Astron. J.* **86**, 1791 (1981); *Astron. J.* **86**, 1825 (1981).
- [14] Y. Sofue and V. Rubin, *Ann. Rev. Astron. Astrophys.* **39**, 137 (2001) [astro-ph/0010594] and references therein.
- [15] W. J. G. de Blok, S. S. McGaugh and V. C. Rubin, *Astron. J.* **122**, 2396 (2001).
- [16] W. J. G. de Blok, S. S. McGaugh, A. Bosma and V. C. Rubin, *Astrophys. J.* **552**, L23 (2001) [astro-ph/0103102].
- [17] W. J. G. de Blok and A. Bosma, *Astron. Astrophys.* **385**, 816 (2002) [astro-ph/0201276].
- [18] S. H. Oh, W. J. G. de Blok, F. Walter, E. Brinks and R. C. Kennicutt, Jr, *Astron. J.* **136**, 2761 (2008) [arXiv:0810.2119].
- [19] S. H. Oh *et al.*, *Astron. J.* **149**, 180 (2015) [arXiv:1502.01281].
- [20] R. A. Swaters, R. Sancisi, T. S. van Albada and J. M. van der Hulst, *Astron. Astrophys.* **493**, 871 (2009) [arXiv:0901.4222].
- [21] W. J. G. de Blok, *Adv. Astron.* **2010**, 789293 (2010) [arXiv:0910.3538].

- [22] A. H. Broeils, *Astronomy and Astrophysics*, **256**, 19 (1992).
- [23] G. Gentile, M. Baes, B. Famaey and K. Van Acoleyen, *Mon. Not. Roy. Astron. Soc.* **406**, 2493 (2010) [arXiv:1004.3421].
- [24] M. Persic, P. Salucci and F. Stel, *Mon. Not. Roy. Astron. Soc.* **281**, 27 (1996) [astro-ph/9506004].
- [25] P. Salucci, *Mon. Not. Roy. Astron. Soc.* **320**, L1 (2001) [astro-ph/0007389].
- [26] A. Borriello and P. Salucci, *Mon. Not. Roy. Astron. Soc.* **323**, 285 (2001) [astro-ph/0001082].
- [27] S. M. Kent, *Astron. J.* **93**, 816 (1987).
- [28] R. Sancisi, *IAU Symp.* **220**, 233 (2004) [astro-ph/0311348].
- [29] M. Verheijen and E. de Blok, *Astrophys. & Space Sci.*, **269**, 673 (1999).
- [30] F. Donato and P. Salucci, *Mon. Not. Roy. Astron. Soc.* **353**, L17 (2004); [astro-ph/0403206].
- [31] S. S. McGaugh, *Galaxies* **2**, 4, 601 (2014) [arXiv:1412.3767].
- [32] F. Lelli, F. Fraternali and M. Verheijen, *Mon. Not. Roy. Astron. Soc.* **433**, 30 (2013) [arXiv:1304.4250].
- [33] R. B. Tully and J. R. Fisher, *Astron. Astrophys.* **54**, 661 (1977).
- [34] S. S. McGaugh, J. M. Schombert, G. D. Bothun and W. J. G. de Blok, *Astrophys. J.* **533**, L99 (2000) [astro-ph/0003001].
- [35] B. Moore, *Nature* **370**, 629 (1994).
- [36] D. N. Spergel and P. J. Steinhardt, *Phys. Rev. Lett.* **84**, 3760 (2000) [astro-ph/9909386].
- [37] M. Kaplinghat, S. Tulin and H. B. Yu, arXiv:1508.03339.
- [38] R. Foot, H. Lew and R. R. Volkas, *Phys. Lett. B* **272**, 67 (1991); R. Foot and R. R. Volkas, *Phys. Rev. D* **52**, 6595 (1995) [hep-ph/9505359].
- [39] R. Foot and R. R. Volkas, *Phys. Rev. D* **70**, 123508 (2004) [astro-ph/0407522].
- [40] R. Foot, *Int. J. Mod. Phys. D* **13**, 2161 (2004) [astro-ph/0407623].
- [41] R. Foot and S. Vagnozzi, *Phys. Rev. D* **91**, 023512 (2015) [arXiv:1409.7174].
- [42] R. Foot, *Int. J. Mod. Phys. A* **29**, 1430013 (2014) [arXiv:1401.3965].
- [43] H. Goldberg and L. J. Hall, *Phys. Lett. B* **174**, 151 (1986).
- [44] A. Ibarra, A. Ringwald and C. Weniger, *JCAP* **0901**, 003 (2009) [arXiv:0809.3196].
- [45] L. Ackerman, M. R. Buckley, S. M. Carroll and M. Kamionkowski, *Phys. Rev. D* **79**, 023519 (2009) [arXiv:0810.5126].

- [46] J. L. Feng, M. Kaplinghat, H. Tu and H. B. Yu, JCAP **0907**, 004 (2009) [arXiv:0905.3039].
- [47] J. Cline, Z. Liu and W. Xue, Phys. Rev. D **85**, 101302 (2012) [arXiv:1201.4858].
- [48] J. Fan, A. Katz, L. Randall and M. Reece, Phys. Dark Univ. **2**, 139 (2013) [arXiv:1303.1521].
- [49] K. Petraki, L. Pearce and A. Kusenko, JCAP **1407**, 039 (2014) [arXiv:1403.1077].
- [50] M. Heikinheimo, M. Raidal, C. Spethmann and H. Veerme, Phys. Lett. B **749**, 236 (2015) [arXiv:1504.04371].
- [51] K. Petraki, M. Postma and M. Wiechers, JHEP **1506**, 128 (2015) [arXiv:1505.00109].
- [52] R. Foot and X. G. He, Phys. Lett. B **267**, 509 (1991).
- [53] B. Holdom, Phys. Lett. B **166**, 196 (1986).
- [54] G. G. Raffelt, Chicago, USA: Univ. Pr. (1996) 664 p; S. Davidson, S. Hannestad and G. Raffelt, JHEP **0005**, 003 (2000) [hep-ph/0001179].
- [55] R. Foot and Z. K. Silagadze, Int. J. Mod. Phys. D **14**, 143 (2005) [astro-ph/0404515].
- [56] R. Foot, Phys. Rev. D **91**, 123543 (2015) [arXiv:1502.07817].
- [57] R. C. Kennicutt, Jr., Astrophys. J. **498**, 541 (1998) [astro-ph/9712213].
- [58] M. Schmidt, Astrophys. J. **129**, 243 (1959).
- [59] W. J. G. de Blok, F. Walter, E. Brinks, C. Trachternach, S. H. Oh and R. C. Kennicutt, Jr., Astron. J. **136**, 2648 (2008) [arXiv:0810.2100].
- [60] R. Foot, Phys. Lett. B **718**, 745 (2013) [arXiv:1208.6022].
- [61] F. Y. Cyr-Racine, R. de Putter, A. Raccanelli and K. Sigurdson, Phys. Rev. D **89**, 063517 (2014) [arXiv:1310.3278].
- [62] Z. Berezhiani, D. Comelli and F. L. Villante, Phys. Lett. B **503**, 362 (2001) [hep-ph/0008105]; A. Y. Ignatiev and R. R. Volkas, Phys. Rev. D **68**, 023518 (2003) [hep-ph/0304260]; Z. Berezhiani, P. Ciarcelluti, D. Comelli and F. L. Villante, Int. J. Mod. Phys. D **14**, 107 (2005) [astro-ph/0312605]; P. Ciarcelluti and Q. Wallemacq, Phys. Lett. B **729**, 62 (2014) [arXiv:1211.5354].
- [63] P. Ciarcelluti and R. Foot, Phys. Lett. B **679**, 278 (2009) [arXiv:0809.4438]; R. Foot, Phys. Lett. B **711**, 238 (2012) [arXiv:1111.6366].
- [64] R. Foot, Phys. Dark Univ. **5-6**, 236 (2014) [arXiv:1303.1727].
- [65] R. Foot, Phys. Rev. D **88**, 023520 (2013) [arXiv:1304.4717].
- [66] R. Foot, JCAP **1412**, 047 (2014) [arXiv:1307.1755].
- [67] R. Foot and Z. K. Silagadze, Phys. Dark Univ. **2**, 163 (2013) [arXiv:1306.1305].

- [68] K. C. Freeman, *Astrophys. J.* **160**, 811 (1970).
- [69] W. J. G. de Blok and S. S. McGaugh, *Mon. Not. Roy. Astron. Soc.* **290**, 533 (1997) [astro-ph/9704274].
- [70] W. J. G. d. Blok, A. Bosma and S. S. McGaugh, *Mon. Not. Roy. Astron. Soc.* **340**, 657 (2003) [astro-ph/0212102].
- [71] G. Gentile *et al.*, *Mon. Not. Roy. Astron. Soc.* **351**, 903 (2004) [astro-ph/0403154].
- [72] S. Salim *et al.*, *Astrophys. J. Suppl.* **173**, 267 (2007) [arXiv:0704.3611].
- [73] J. C. Lee *et al.*, *Astrophys. J. Suppl.* **192**, 6 (2011) [arXiv:1009.4705].
- [74] I. D. Karachentsev and E. I. Kaisina, *Astron. J.* **146**, 46 (2013) [arXiv:1305.4791].
- [75] D. C. Martin *et al.*, *Astrophys. J.* **619**, L1 (2005) [astro-ph/0411302].
- [76] K. A. Herrmann, D. A. Hunter and B. G. Elmegreen, *Astron. J.* **146**, 104 (2013) [arXiv:1309.0004].
- [77] I. D. Karachentsev, V. E. Karachentseva, W. K. Huchtmeier and D. I. Makarov, *Astron. J.* **127**, 2031 (2004). I. D. Karachentsev, D. I. Makarov and E. I. Kaisina, *Astron. J.* **145**, 101 (2013) [arXiv:1303.5328].
- [78] K. B. W. McQuinn *et al.*, *Astrophys. J.* **724**, 49 (2010) [arXiv:1009.2940].
- [79] A. Gil de Paz *et al.*, *Astrophys. J. Suppl.* **173**, 185 (2007) [astro-ph/0606440].
- [80] M. J. Meyer, M. A. Zwaan, R. L. Webster, S. Schneider and L. Staveley-Smith, *Mon. Not. Roy. Astron. Soc.* **391**, 1712 (2008).